International Symposium
On Turbulence and Shear Flow
Phenomena (TSFP-9)
June 30 - July 3, 2015 *Melbourne, Australia*

AN INVESTIGATION OF SONIC & SUPERSONIC AXISYMMETRIC JETS: CORRELATIONS BETWEEN FLOW PHYSICS AND FAR-FIELD NOISE

Andrew S. Magstadt, Matthew G. Berry, Zachary P. Berger, Patrick R. Shea, and Mark N. Glauser
Dept. of Mechanical & Aerospace Engineering
Syracuse University
Syracuse, NY 13244
asmagsta@syr.edu, mgberry@syr.edu, zpberger@syr.edu, prshea@syr.edu, mglauser@syr.edu

Christopher J. Ruscher, Sivaram Gogineni
Spectral Energies, LLC.
Dayton, OH 45431
christopher.ruscher.ctr@us.af.mil, sgogineni@spectralenergies.com

ABSTRACT

An axisymmetric convergent jet is studied at ideal and underexpanded conditions using velocity and acoustic data. Time-resolved and large-window PIV capture near-field velocities and are simultaneously sampled with far-field microphones. POD is used to extract modes representative of physical processes in the flow. Specifically, screech-containing and turbulent mixing modes are isolated in the supersonic case. The decoupled velocity fields are then correlated with acoustic data to identify modes related to specific noise spectra. Finally, selective flow reconstruction is carried out to reduce flow features associated with an imperfectly expanded jet.

INTRODUCTION

Understanding and reducing jet noise are difficult problems due to the inevitable turbulence encountered. The aerospace industry continues to invest considerable effort into mitigating jet noise as it creates unwanted acoustic pollution near airports, generates negative health consequences to flight deck crews, and compromises the stealth of military aircraft. Today, supersonic flight is becoming a standard for military aircraft and is being revisited for commercial applications. Furthering the understanding of turbulence in supersonic flow is a critical step towards noise source identification and suppression for future aircraft.

While research in the area of aeroacoustics has progressed considerably since its introduction, Tam (1998), engine technologies are advancing at increasing rates, which push aircraft to greater speeds. Advanced designs utilize exotic nozzle and flow configurations to increase performance and abate noise generation in supersonic jets, Henderson *et al.* (2012). However, many of the heuristic solutions employed to date have been guided by partially anecdotal evidence, leaving incomplete understanding of the fluid mechanics involved. Prior to studying such configurations, the axisymmetric nozzle is revisited to interpret shock-turbulence interactions as anticipated in future designs. This prompted an investigation of supersonic noise generation in Syracuse University's anechoic chamber.

Current research is focused on identifying important flow features in a cold, axisymmetric convergent jet; in particular, sonic and supersonic flows are investigated to further recognize differences in noise generation associated with shocks. Particle imaging velocimetry (PIV) is simultaneously sampled with far-field pressures to allow for rigorous analyses. Reduced-order modeling (e.g. POD) of the jet plume in the streamwise plane (complementing work by Caraballo *et al.* (2003)), directivity and magnitude calculations of acoustic radiation, and correlations between the two measurements are carried out. Flow physics are then related to far-field noise signatures. Previously, subsonic test campaigns at Syracuse University's Skytop Turbulence Laboratory by Low *et al.* (2013) and Berger *et al.* (2014) have presented evidence correlating deterministic spatial structures in the near-field flow with far-field noise. At present, data sets containing ideally and underexpanded jets ($M_j = 1.0$ & $M_j = 1.1$) are presented to similarly locate noise generation mechanisms.

EXPERIMENTAL SETUP

The experimental results were acquired in the Skytop Turbulence Laboratory at Syracuse University. The 206 m^3 anechoic chamber is acoustically treated with fiberglass wedges, achieving a cutoff frequency of 150 Hz. Within the chamber is an axisymmetric 5^{th}-order-polynomial convergent nozzle ($M_d = 1.0$) with a diameter of $D = 50.8mm$, described by Tinney *et al.* (2004). For the $M_j = 1.0$ and $M_j = 1.1$ test cases discussed below, $Re = 1.1 \cdot 10^6$ and $Re = 1.2 \cdot 10^6$, respectively, are sustained. The anechoic chamber and jet can be seen in Figure 1.

Particle Image Velocimetry

Near-field velocity measurements were acquired using two different PIV setups. A time-resolved PIV (TRPIV) system was used to gather the $M_j = 1.0$ data. This system was unavailable when the $M_j = 1.1$ test campaign was underway, thus large-window PIV (LWPIV) was utilized to capture data for the supersonic case.

The TRPIV system operates a 10 kHz Quantronix Hawk-Duo Nd:YAG laser. In combination with a Photron

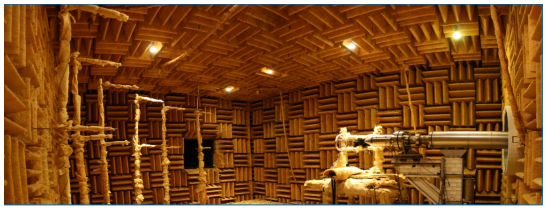

Figure 1. Anechoic chamber showing far-field microphone array (left), near-field pressure ring and PIV instrumentation (center), and axisymmetric jet (right).

FASTCAM CCD, two-component velocity measurements were taken along the jet centerline (i.e. the $r-z$ plane) in approximately 1.5 x 1.5 diameter separate windows. Samples were acquired from $(z/D=0)$ to $(z/D=7.8)$ downstream with 0.5 diameter overlap. The LWPIV utilized a standard 4 Hz New Wave Nd:YAG Gemini laser that triggered three Dantec HiSense cameras simultaneously. The laser sheet and cameras were oriented to take two-component measurements along the centerline of the jet axis. Each camera's field of view slightly overlapped the neighboring one's to ensure appropriate merging of velocity vectors. Using a least squares algorithm as described in Shea *et al.* (2014), the PIV images were stitched together to achieve a single streamwise velocity window from $2.5 < z/D < 9.4$ and $-1.0 < r/D < 1.0$.

Proper Orthogonal Decomposition (POD) is a method for decomposing a flow into its energetic building blocks first introduced by Lumley (1967). Sirovich (1987) made the POD method more tractable for data with large spatial resolution, such as PIV, and is the method used in this paper. The decomposition give spatial modes, $\phi_i^{(n)}(\vec{x})$, and temporal coefficient, $a_n(t)$, which allow the reconstruction of the flow using

$$u_i(\vec{x},t) = \sum_{n=1}^{N} a_n(t)\phi_i^{(n)}(\vec{x}). \quad (1)$$

Far-field Acoustics

Far-field acoustics were simultaneously sampled with each PIV setup. The setup uses two arrays of six G.R.A.S. free-field condenser microphones positioned in an arc, $(z/D=75)$ away from the nozzle lip. One arc of six microphones is located in-plane with the jet (as shown in Figure 1), while the second arc is positioned approximately one meter above, angled down at 15°. The microphones are spaced in 15°increments from 90°to 165°with respect to the jet axis, where the jet axis, $+z$, corresponds to 180°.

National Instruments' PXI and SCXI systems were used for synchronization and acoustic data acquisition. Upon test initialization, PIV triggers were sampled and used to match the appropriate acoustic signatures for data analysis. The number and frequencies of PIV snapshots and microphone samples (found in Table 1) were determined by hardware restrictions and run times. TRPIV experiments were limited to less than one second (due to bandwidth limitations from the large amount of data acquired), while the LWPIV setup allowed for much longer simultaneous acoustic sampling. TRPIV offers great temporal resolution, but sacrifices the field of view due to large laser power requirements. LWPIV can capture a much greater interrogation region, but does not contain useful temporal information for this flow.

Table 1. Data acquisition parameters.

M_j	f_{PIV}	N_{PIV}	f_{Mic}	N_{Mic}
1.0	10 kHz	8623	40 kHz	$4x10^5$
1.1	4 Hz	2500	25 kHz	$2.5x10^7$

With the time-varying component of the modal decomposition calculated, $a_n(t)$, cross-correlations can be computed to relate the simultaneously sampled far-field noise$P_i(t)$ to each spatial mode. This is accomplished by creating a range of time lags, τ, around the average acoustic propagation time (approximately 10 ms) and generating a correlation matrix for each time lag, microphone, and mode number. The maximum correlation values in each time lag series are then extracted for relation to flow physics.

RESULTS

Ideally Expanded Jet

The data from the $M_j = 1.0$ case was originally reported by Berger *et al.* (2012). Here, important results are summarized. Averaged velocities from four (of seven) camera locations are shown in Figure 2. Since the data are not phase-locked, a merged instantaneous flow-field is not possible. Initial analyses were thus focused on the velocity fields from individual camera locations.

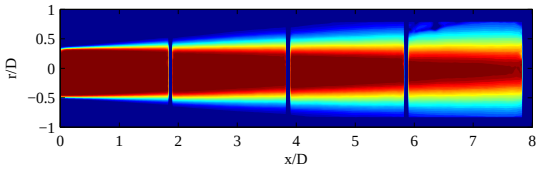

Figure 2. Ensemble average of time-resolved data from four separate camera locations. An additional three locations were taken, to give overlap of each flow-field.

The final camera location of the TRPIV setup, $6 < z/D < 7.8$, is selected to investigate since much evidence has been found to suggest a major source of noise is near the collapse of the potential core (e.g. Seiner (1998) and Hall (2008)). Snapshot POD is applied as a reduced-order model. The resulting streamwise POD modes are shown in Figure 3. These first 18 modes possess 45 % of the data's energy. Modes 1 & 2 contain large structures, indicative of the greatest coherent structures. As the subsequent less energetic modes are examined, the structures begin to breakdown. The symmetric modes (i.e. 3-6) are likely associated with column modes in the jet ($m=0$ in the $r-\theta$ plane). The even less dynamical modes lose symmetry and the smaller structures become more poorly organized (e.g. 9-14), presumably capturing the collapsing mixing layers which introduce further turbulence in the center of jet. Thus, it is believed that these higher modes are responsible for much of the acoustic radiation propagated to the far field.

Far-field data are next consulted. Spectral content are not of particular interest for the $M_j = 1.0$ case, but may be found in the report by Berger *et al.* (2012). Typical acoustic signatures were observed, with turbulent mixing being the prime source of noise and spatially-varying magnitudes

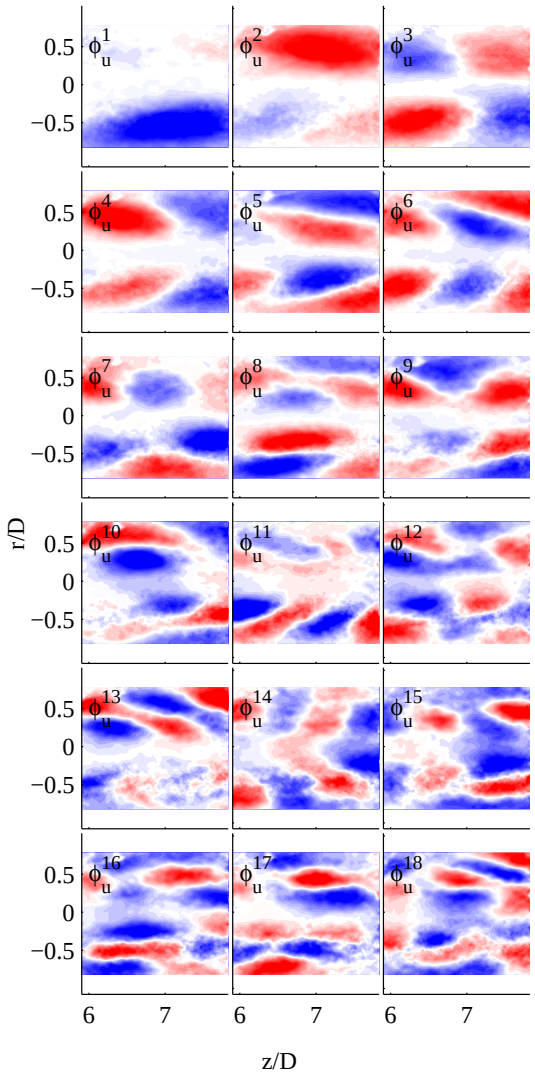

Figure 3. First spatial modes of the $M_j = 1.0$ data, taken near the collapse of the PC.

obeying refraction Atvars *et al.* (1965). However, the time-varying pressure signals were used to compute correlations. As discussed in the Experimental Setup section, correlations can be computed to draw conclusions between the spatial functions and far-field acoustics. Calculations of such yielded significance between a select few modes and the 165°microphone, shown in Figure 4. Specifically, modes 15 & 16 are found to have the greatest correlations, consistent with the findings of Berger *et al.* (2012). The isolation and control of these "loud" modes is then used in attempts to reduce the noise. No other outstanding correlations were found at other microphones.

Underexpanded Jet

The multiple-camera setup of the LWPIV captures phase-locked velocity data at three separate location and allows the merging of instantaneous vector fields. Figure 5 shows a snapshot of the jet's streamwise instantaneous (*a*), mean (*b*), and centerline (*c*) velocities. Fluctuating mean velocities indicate the existence of shock cells typical of

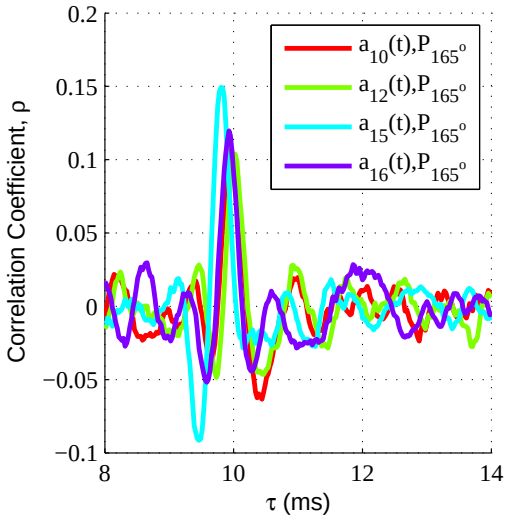

Figure 4. Loud modes at the 165°microphone.

underexpanded jets. The jet is then further analyzed via a reduced order model.

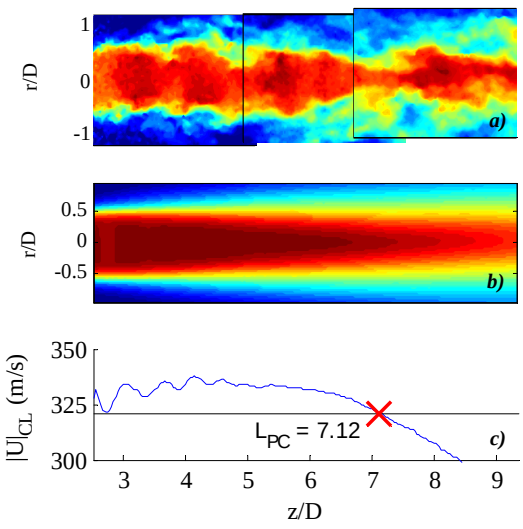

Figure 5. Streamwise velocity component of the $M_j = 1.1$ jet. Separate instantaneous flow-fields (*a*) are merged and averaged (*b*), and the centerline velocity is then extracted (*c*) to illustrate shock cells and define the potential core length.

POD is again implemented and the velocity is decomposed into basis functions. The most energetic of these spatial modes are found in Figure 6. Some distinct features of the jet are highlighted in these spatial modes, and they are classified into three main groups based on specific energy content and shape. The lowest modes (1-3) exhibit large-scale structures near the collapse of the potential core, modes 6-9 possess strong streamwise oscillations within the supersonic core, and the higher modes (i.e. 11-14 & 17-20) contain smaller organized structures embedded in the mixing layers. Each group is believed to be associated with a particular physical feature of underexpanded flow. Modes

15 & 16 appear to capture smaller events at the collapse of the potential core. The unmentioned eigenfunctions are to thought to be transitional states and may or may not be mathematical constructs necessary to satisfy the equations.

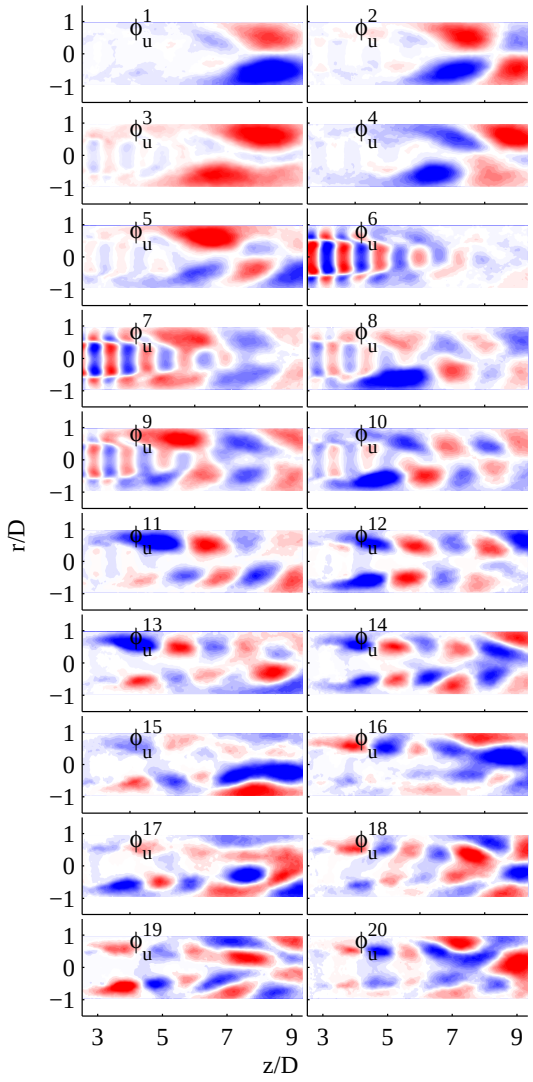

Figure 6. First spatial modes of the $M_j = 1.1$ data.

The first modes of Figure 6 are now discussed in detail. Near the collapse of the potential core, vortices breakdown (from mode $1 \rightarrow 2$), a wave-like feature is found and the vortices *increase* in size (mode 3), followed by further vortex breakdown (mode $3 \rightarrow 5$). The enlarged length scale found in mode 3 is atypical, as structures in isotropic homogeneous turbulence should be less energetic with decreasing size. Many jet flow models have been nominated over the years to describe large-scale structure, but two particular theories match well the results here. Bishop *et al.* (1971) found experimental evidence of large-scale eddies, i.e. larger than the width of the shear layer, oscillating near the collapse of the potential core in a manner similar to instabilities found in laminar flow. A separate model proposed by Tam (1972) suggests helical instabilities of the jet structure resonate with the shock disturbances, resulting in noise generation through the oscillation of the jet and unsteady entrainment. Both theories offer reasonable explanations.

Regions of compression and decompression are thought to be associated with the shock cell-like modes 6-9. Fluctuating velocities contained within the potential core are apparently tied to axisymmetric structures in the shear layer, likely vortex rings. Dominant wavenumbers are calculated in the shear layer and potential core as $\nu = 18.6m^{-1}$. Based on a local wavespeed of $(c - u_{conv})$, where u_{conv} is taken in the shear layer to be $114m/s$, these lead to an average frequency of 4550 Hz. As will be seen, this is close to the fundamental screech frequency. Additionally, the vortex rings are almost exactly 180°out of phase with the potential core fluctuations, suggesting that the vortices are driven by their adjacent downstream shock. These interactions at least partially illustrate the feedback mechanism responsible for screech tones Tam (1995). The slower-convecting shear layer acts as a waveguide and allows Mach wave radiation at specific frequencies, generated from vortex-shock interactions, to propagate upstream to the nozzle lip.

Finally, the mixing layer modes ($n > 10$) capture smaller eddies. Specific spatial functions qualitatively match well with the lower modes of subsonic jets Berger (2014), and are believed to be associated with turbulent mixing noise as in the $M_j = 1.0$ case. More evidence is sought to reinforce the relations to noise production, hence the far-field noise data are next considered.

The acoustic spectra of the $M_j = 1.1$ are presented in Figure 7 as contours in polar coordinates. Sound pressure levels (SPLs) are plotted as a function of Strouhal number ($St = \frac{fD}{U_j}$) and microphone angle relative to the jet. Supersonic noise is well documented, see Tam (1995), and the results found here are consistent with previous findings. Narrow bands of intense SPLs (e.g. $St \sim 0.6$) are identified as screech tones ($f_{s_0} = 4545Hz$ & $f_{s_1} = 9101Hz$), the peak from $0 < St < 0.3$ and directed towards the shallow microphones is characteristic of turbulent mixing, and the weak gradients from 150°to 120°extending across a range of St are considered to be associated with broadband shock-associated noise (BBSAN). For this jet, the BBSAN is weak and thus does not show up strongly in the spectra.

As with the $M_j = 1.0$ data, correlation coefficients are computed for each microphone, POD mode, and time lag. In contrast to the sonic case though, the underexpanded jet has significant correlations at multiple microphones. To display the multidimensional data, the maximum values of the correlations are plotted in Figure 8. The orientation is the same as the frequency spectra presented in Figure 7, with the radial coordinate exchanged for the normalized cross-correlation coefficient.

Figure 8 demonstrates the directional dependence of the most highly connected velocity-acoustic correlations. A threshold of $\rho > 3\sigma$ was chosen as the minimum value of significance, where σ is the standard deviation of the maximum correlation coefficients. Comparing Figures 6, 7, and 8, one can immediately see which modes overlap particular noise signatures. The high correlation coefficients of the shock-containing modes (6-9) align with the screech tone propagation to the microphones at 90°, 105°, and 165°. While the fundamental screech frequency is greater at the shallower angle, the presence of the 1st at the 90°and 105°microphones apparently results in higher correlations. This provides additional evidence that modes (6-9)

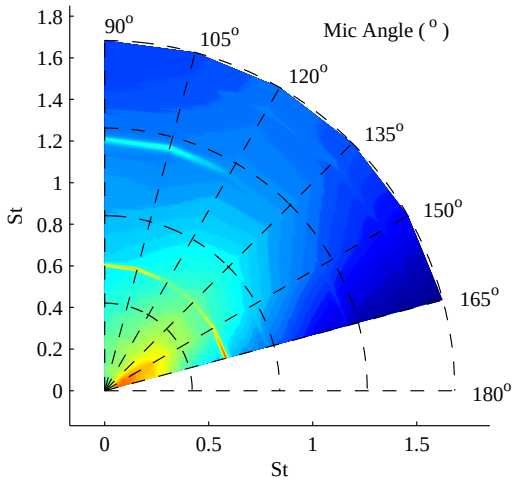

Figure 7. Frequency and directional dependence of SPLs for $M_i = 1.1$. The max intensity is approximately $80 dB/Hz$.

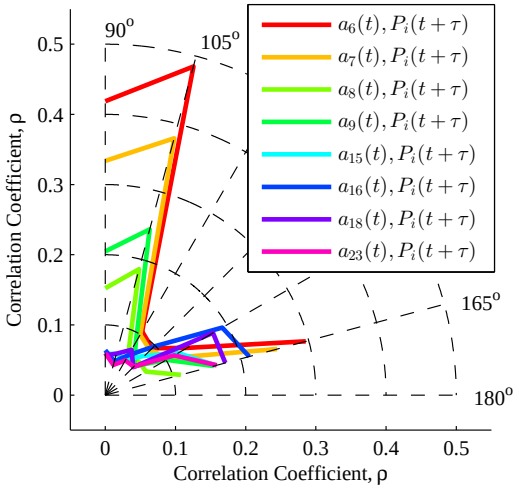

Figure 8. Directional dependence of the maximum velocity-acoustic correlations for $M_j = 1.1$.

correspond to screech production. The angles where turbulent mixing noise exist (i.e. 150°and 165°) also have high correlations to the lower energy modes ($n = 15, 16, 18$ and 23), associated with the collapse of the potential core. This evidence is in good agreement with countless research on subsonic axisymmetric jets, where turbulent mixing is the primary component of noise generation and propagates into the cone of coherence, Atvars *et al.* (1965) and Tam (1998). Though not presented, data collected from a second microphone array (positioned above the one shown in Figure 1) are consistent with the current results. Regions of higher and lower acoustic patterns in the offset array result in the expected change in correlation coefficients.

Similarities across Mach numbers

Comparison between the two cases is difficult due to differences in instrumentation used, as discussed by Berry *et al.* (2015). However, some similarities are expected in flow structure and noise generation. To make such a comparison, the LWPIV data must be truncated and interpolated to match the spatial locations of the TRPIV data before executing POD. This is done on the flow field, and the principal modes are then compared via a spatial cross-correlation coefficient between the LWPIV and truncated LWPIV. These data are omitted for brevity, but the large-scale structure are, not surprisingly, lost in the operation of truncation. The higher modes of the LWPIV, however, correlate to the lower modes of the truncated data (e.g. modes 23 and 10), consistent with the window dependent relations found by Shea *et al.* (2014) and Berry *et al.* (2015). Screech modes' (6-9) correlation to the far-field noise are entirely lost due to the truncation process at this location, but turbulent mixing remain. These newly computed eigenfunctions are then compared to the $M_j = 1.0$ jet.

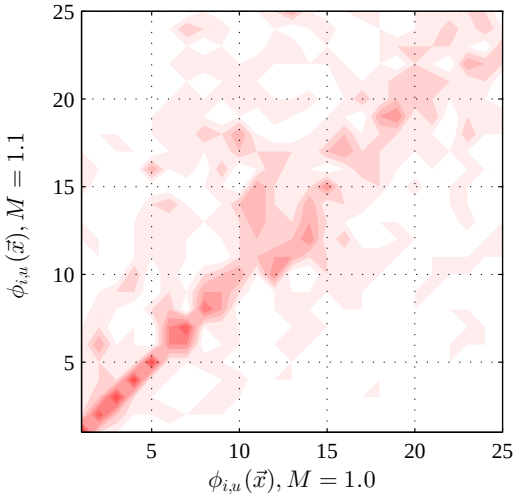

Figure 9. Spatial correlation between the first modes of $M_j = 1.0$ and the truncated $M_j = 1.1$ data at $6 < z/D < 7.8$. Contours range from no correlation (white) to highly correlated (dark red).

Figure 9 demonstrates the similarity of the lowest modes. The spatial mode switching observed also matches the recomputed velocity-acoustic correlations. Mode 10 of the $M_j = 1.1$ coincides spatially well with mode 12 of $M_j = 1.0$, and both show significant correlations to the microphone at 165°. Similarly, modes 12 & 14 interchange, 15 remains the same, and 17 & 16 reciprocate. Each has a far-field correlation coefficient, $\langle a_n(t), P_i(t+\tau)\rangle$, close to that of its partner. This suggests similar events are recurrent across the two different Mach numbers and are captured by unique POD modes. Some further, qualitative, verification is found through the reconstruction of the velocity fields.

By removing the screech-containing modes, the remaining modes (shown to be highly spatially-correlated to the sonic case) ought to reproduce a flow-field similar to the $M_j = 1.0$ jet. Figure 10 shows instantaneous flow fields from the $M_j = 1.0$ case using reconstructed TPRIV data, *(a)*, and the $M_j = 1.1$ data as produced from selective reconstruction of the LWPIV *(b)*, where modes 6-9 have been omitted. The TRPIV data uses velocity information from seven different cameras and merges the fields together through a POD modal basis, discussed in a paper by Berger

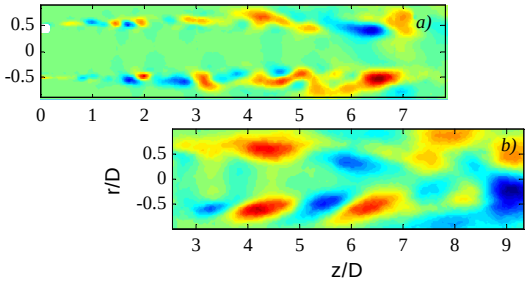

Figure 10. Reconstruction of fluctuating velocities for snapshots of *(a)* $M_j = 1.0$ from TRPIV data and *(b)* $M_j = 1.1$ from LWPIV data with the shock modes omitted.

et al. (2014). The chart used, *(a)*, is borrowed from this work. Identical matching would be lucky given the nature of turbulence, yet similarities between the two data sets do exist such as activity near the potential core. Most importantly, shock-related features of the underexpanded jet are almost entirely absent. Vortices clustered around the collapse of the potential core and located in the shear layer are essentially all that remain, akin to a sonic or subsonic jet.

CONCLUSIONS

POD and velocity-acoustic correlations have been carried out on data taken from an axisymmetric jet operating at ideal and underexpanded conditions. Specific POD modes were found to contain important physics of the problem. Specifically the large-scale structure of the jet, shock-related fluctuations, and turbulent mixing regions of the flow were isolated through POD in the supersonic case. By computing cross correlations, particular modes were found related to noise spectra. Strong evidence links modes 6-9 to screech production. Velocity-acoustic correlations associate these modes with the tonal patterns, and the spatial analysis suggests that vortex-shock interactions produce Mach waves which can propagate upstream through the shear layer at screech frequencies. Additionally, turbulent mixing noise was isolated. By comparing to the sonic case, where turbulent mixing is the sole source of noise, similar mode shapes were found across both Mach numbers.

The distinct features of supersonic flow create an opportunity to classify particular sources of acoustic spectra through reduced-order models. For example, POD modes 15 and 16 of the TRPIV and truncated LWPIV data sets presented herein appear to represent structures indicative of noisy turbulent flow events. These occur near the collapse of the potential core, yet the cause of such events may be elsewhere in the flow. Time-resolved data allows one to watch the evolution of the flow and identify a particular event. The large-window can then be looked at using similarities between POD modes to learn more about the flow and ascertain the behavior of the more energetic modes which may influence the loud modes. Insight into screech production is believed to have increased, but the cause for noisy turbulent events remains under investigation.

ACKNOWLEDGMENTS

Thanks are given to Spectral Energies, LLC. and AFRL, with Dr. Barry Kiel as project monitor, for the continued support in this research.

REFERENCES

Atvars, J, Schubert, LK, Grande, E & Ribner, HS 1965 *Refraction of sound by jet flow or jet temperature*. Institute for Aerospace Studies, University of Toronto.

Berger, Z.P., Berry, M.G., Shea, P.R., Glauser, M.N., Jiang, N., Noack, B.R., Gogineni, S., Kaiser, E. & Spohn, A. 2014 Analysis of high speed jet flow physics with time-resolved piv. *52nd AIAA Aerospace Sciences Meeting* (1226).

Berger, Z.P., Low, K.R., Kostka, S., Gogineni, S. & Glauser, M.N. 2012 Investigation of an axisymmetric transonic jet with high resolution time-resolved piv. *48th AIAA Joint Propulsion Conference* (3822).

Berger, Zachary P 2014 The effects of active flow control on high-speed jet flow physics and noise. PhD thesis, Syracuse University.

Berry, M. G., Magstadt, A. S., Berger, Z. P., Shea, P. R., Glauser, M. N., Ruscher, C. J. & Gogineni, S. P. 2015 Comparison of spatial and temporal resolution on high speed axisymmetric jets. *53rd AIAA Aerospace Sciences Meeting* .

Bishop, K A, Williams, Ffowcs & Smith, W 1971 On the noise sources of the unsuppressed high-speed jet. *Journal of Fluid Mechanics* .

Caraballo, E., Samimy, M. & Scott, J. 2003 Application of proper orthogonal decomposition to a supersonic axisymmetric jet. *AIAA Journal* .

Hall, A. M. 2008 An experimental investigation of low-dimensional techniques for large scale noise source characterization in a heated jet. *Ph.D. dissertation, Syracuse University* .

Henderson, B., Bridges, J. & Wernet, M. 2012 Jet noise reduction potential from emerging variable cycle technologies. *48th AIAA Joint Propulsion Conference* .

Low, K.R., Berger, Z.P., Kostka, S., El Hadidi, B., Gogineni, S. & Glauser, M. 2013 A low-dimensional approach to closed-loop control of a mach 0.6 jet. *Experiments in Fluids* pp. 1–17.

Lumley, J. L. 1967 The structure of inhomogeneous turbulent flows. *Atm. Turb. and Radio Wave Prop. ed. by A.M. Yaglom and V. I. Tatarsky, (Nauka, Moscow)* pp. 166–178.

Seiner, J. M. 1998 A new rational approach to jet noise reduction. *Theoretical and Computational Fluid Dynamics* **10** (1-4), 373–383.

Shea, P.R., Berger, Z.P., Berry, M.G., Gogineni, S. & Glauser, M.N. 2014 Low-dimensional modeling of a mach 0.6 axisymmetric jet. *52nd AIAA Aerospace Sciences Meeting* (0245).

Sirovich, L. 1987 Turbulence and the dynamics of coherent structures, part i,ii, and iii. *Quarterly Applied Mathematics* **45**.

Tam, C. K. 1972 On the noise of a nearly ideally expanded supersonic jet. *Journal of Fluid Mechanics* **51**, 69–95.

Tam, C. K. 1995 Supersonic jet noise. *Annu Rev of Fluid Mech* .

Tam, C. K. 1998 Jet noise: Since 1952. *Theoretical and Computational Fluid Dynamics* **10** (1-4), 393–405.

Tinney, C. E., Hall, A. M., Glauser, M. N.and Ukeiley, L. S. & Coughlin, T. 2004 Designing an anechoic chamber for the experimental study of high speed heated jets. *42nd AIAA Aerospace Sciences Meeting and Exhibit* (0010).